Quarterly Progress Report

N01-NS-1-2333

Restoration of Hand and Arm Function by Functional Neuromuscular Stimulation

Period covered: June 1, 2001 to June 30, 2001

Principal Investigator: Robert F. Kirsch, Ph.D.

Co-Investigators:

Patrick E. Crago, Ph.D.
P. Hunter Peckham, Ph.D.
Warren M. Grill, Ph.D.
J. Thomas Mortimer, Ph.D.
Kevin L. Kilgore, Ph.D.
Michael W. Keith, M.D.
David L. Wilson, Ph.D.
Joseph M. Mansour, Ph.D.
Jeffrey L. Duerk, Ph.D.
Wyatt S. Newman, Ph.D.
Harry Hoyen, M.D.
John Chae, M.D.
Jonathon S. Lewin, M.D.
Richard Lauer, Ph.D.

Case Western Reserve University
Wickenden 407
10900 Euclid Avenue
Cleveland, OH 44106-7207
216-368-3158 (voice)
216-368-4969 (FAX)
rfk3@po.cwru.edu

Contract abstract

The overall goal of this contract is to provide virtually all individuals with a cervical level spinal cord injury, regardless of injury level and extent, with the opportunity to gain additional useful function through the use of FNS and complementary surgical techniques. Specifically, we will expand our applications to include individuals with high tetraplegia (C1-C4), low tetraplegia (C7), and incomplete injuries. We will also extend and enhance the performance provided to the existing C5-C6 group by using improved electrode technology for some muscles and by combining several upper extremity functions into a single neuroprosthesis. The new technologies that we will develop and implement in this proposal are: the use of nerve cuffs for complete activation in high tetraplegia, the use of current steering in nerve cuffs, imaging-based assessment of maximum muscle forces, denervation, and volume activated by electrodes, multiple DOF control, the use of dual implants, new neurotization surgeries for the reversal of denervation, new muscle transfer surgeries for high tetraplegia, and an improved forward dynamic model of the shoulder and elbow. During this contract period, all proposed neuroprostheses will come to fruition as clinically deployed and fully evaluated demonstrations.

Summary of activities during this reporting period

The starting date of this contract was June 1, 2001, so this report covers the activities only for one month, from June 1 – 30, 2001.

The following activities are described in this report:

- *Evaluation of control sources to restore arm function via FNS to individuals with high level tetraplegia (C3-C4 SCI).*
- *Development of EMG-based controller strategies for restoring hand grasp in individuals with low-level tetraplegia (C7 SCI).*
- *Measurement of human upper extremity nerve diameters and branch-free lengths.*
- *Magnetic resonance imaging of muscles of the human elbow and shoulder.*

Evaluation of control sources to restore arm function via FNS to individuals with high level tetraplegia (C3-C4 SCI)

Contract section: E.1.a.iv Command sources for high tetraplegia

Abstract

The purpose of this study is to develop a user interface to an advanced neuroprosthetic system that will be used to restore upper extremity function to individuals with high tetraplegia resulting from a spinal cord injury at or above the fourth cervical level (C3-C4). These individuals retain voluntary control over the muscles of the head and neck, but have complete paralysis of both upper and lower extremities. The goal of this project is to determine the most appropriate method of enabling these individuals to control the movement of their arm and hand. The outcome of this project, a neuroprosthetic control algorithm for high level tetraplegia, will be combined with the outcome of the arm movement and coordination projects to produce a complete neuroprosthetic system

Methods

Work was initiated during this first quarter on the robotics component of this program. The objective of this task is to create a system that can emulate the kinematics and dynamics of a human arm under FNS control. The intent is to be able to emulate candidate controllers prior to the implementation of a full neuroprosthesis in individuals with high tetraplegia, enabling faster evaluations of a larger number of proposed controllers using able-bodied subjects.

For this evaluation, a Kawasaki JS-10 robot is being used. As with all industrial robot designs, this robot is an imperfect match for the kinematics and dynamics of a human arm. Specifically, it has only 6 degrees of freedom (only two of which are at the shoulder), it is overly long relative to human scale, and it has higher weight and inertia and lower accelerations than a human arm. However, the arm will be mounted horizontally with its base at shoulder height, enabling an approximation to human arm mobility. Further, computer controls for the robot are being designed to have the arm track a model-reference controller based on human-arm dynamics, prospectively producing human-like dynamics. Unusual among industrial robots, this machine has been retrofitted with an open-architecture controller with high-speed access directly to motor torques. Further, the robot has been instrumented with a 6-dof force/torque wrist sensor with high-speed, low-latency interface to the control computer. These features are crucial to accomplishing the project goals.

Results

During this first quarter, preparations have begun in parallel on the critical tasks. Gravity loads and maximum torque capacities were characterized, resulting in the conclusion that the (highly unusual) proposed mounting orientation will be feasible within the robot's torque constraints. Subsequently, an initial design for the robot mounting stand and safety shield was roughed out. Further, an EMG amplifier was interfaced to the robot controller, and primitive EMG-based robot motion command capability was demonstrated.

Next Quarter

During the next quarter, the test stand design will be detailed and fabrication will begin. Robot control via EMG signals will be further developed. The first (primitive) control algorithms will be attempted on the robot. Model reference dynamic tracking control will be initiated.

Development of EMG-based controller strategies for restoring hand grasp in individuals with low level tetraplegia (C7 SCI)

Contract section: E.1.b Control of Grasp Release in Lower Level Tetraplegia

Abstract

The purpose of this project is to develop and evaluate an advanced neuroprosthesis to restore hand function in persons with C7 (OCu:5 to OCu:7) level injuries. Through this work, we will implement in human subjects a control methodology utilizing myoelectric control from synergistic muscles to govern the activation of paralyzed muscles of the forearm and hand that can be stimulated to contract. This work encompasses the following objectives:

1) Demonstrate the feasibility of acquiring myoelectric signals that are appropriate for controlling the neuroprosthesis

2) Develop and test control algorithm options using a simulated neuroprosthesis controller
3) Implement myoelectric control of the hand grasp neuroprosthesis in two subjects with C7 level spinal cord injury and evaluate hand performance.

Methods and Results

During this quarter, work has begun to establish the signal acquisition and processing techniques to be used during experiments. Protocols for testing the ability of a subject to generate repeatable signals having consistent amplitude and frequency characteristics are being designed. The problem of stimulation artifact in the myoelectric signals has also been investigated and a method to eliminate it has been tested. Finally, some initial feasibility studies of control algorithms have been implemented as computer simulations.

Signal Acquisition and Processing

The laboratory setup for recording and processing myoelectric signals consists of recording electrodes, hardware for signal amplification, filtering, and digitization, as well as software for real-time digital signal processing. Surface electrodes (1-cm, self-adhesive, Kendall-LTP) and fine-wire bipolar percutaneous intramuscular electrodes (Nicolet Biomedical, Inc.) are being used to record EMG signals during this phase of the work. The signal is amplified by a factor of 1000 to 3000, filtered with a pass band of 100 to 1000 Hz, and sampled at 2000 Hz using a 16-bit ADC (PCI-6052E, National Instruments Corp.). The digitization, processing, and display of the signals are controlled by custom routines written with the LabView ™ software package.

Several different methods for processing the digitized signal as it is acquired have been implemented. Signal amplitude was estimated in three ways: 1) low pass filtering with a 2 Hz cutoff, computing the root mean square (RMS), and 3) the mean absolute value (MAV) during successive epochs of signal. Frequency content was estimated in two ways: 1) computing the variance (VAR) and the 2) number of zero-crossings (ZC) during successive epochs of signal. These signal processing techniques were implemented in LabView™ so that the raw and processed signal could be displayed in real-time on the computer screen, as shown in Figure 1.

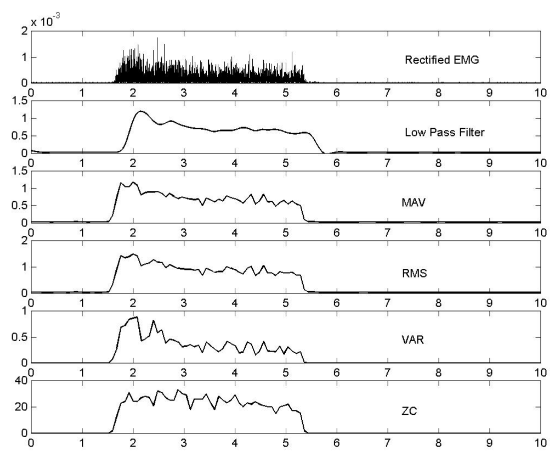

Figure 1: Signal processing methods

Characterizing Voluntary Contractions

Protocols are being established for testing the ability of a subject to modulate myoelectric activity in a pair of muscles that will allow synergistic control. In C7 spinal cord injury, the strongest muscles that also function synergistically with hand function are the wrist flexors (flexor carpi radialis, FCR), and wrist extensors (extensor carpi radialis longus and brevis, ECRL and ECRB). Therefore, our initial work is focusing on these muscles as control sources, although the finger extensors may also be strong enough in some individuals for this purpose. Experiments will be conducted to 1) determine the baseline activity in the control muscles, 2) evaluate the ability of the subject to produce repeatable transient and sustained contractions, and 3) examine the co-contraction characteristics of the two myoelectric signals. The signal characteristics defined through these experiments will be necessary for the development of suitable subject-specific control algorithms.

Surface electrodes were placed over the FCR and ECRL/B of an able-bodied subject and the myoelectric signals were recorded while the subject generated two levels of sustained contraction from both muscles. First, the subject was instructed to generate ten low –level contractions of the ECR, each contraction lasting about 3 seconds and separated by 2 seconds of rest. The same was repeated for the FCR. Then ten high-level contractions of both muscles were recorded. The subject was instructed to be as consistent as possible when making his contractions, but no visual feedback of the recorded signal was provided. Figure 2 shows the MAV signals of both ECR and FCR during one contraction of each of the four contraction conditions (low ECR, high ECR, low FCR, high FCR). This figure shows that the subject is able to generate high and low ECR signals that appear distinct from one another. He likewise can generate apparently distinct high and low FCR signals. The levels of co-contraction in the antagonist muscles are also shown during the intended agonist contractions. The level of the intended contraction appears to be always greater than the level of co-contraction by the agonist.

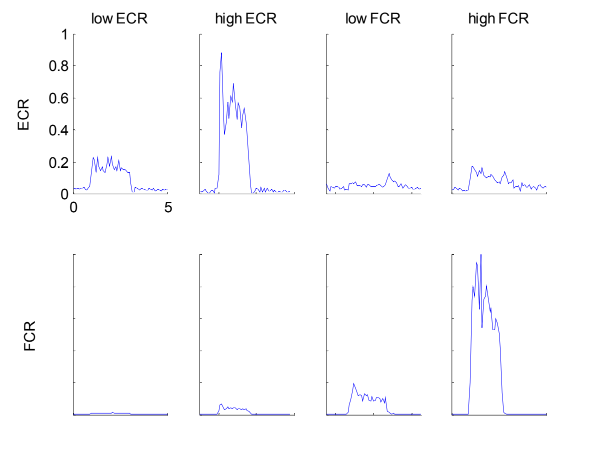

Figure 2: Issuing of high and low signals from ECR and FCR

To verify these qualitative observations of one set of contractions, the means of the MAVs representing each contraction were calculated and are shown in Figure 3 for the ECR and FCR during their respective intended contractions (co-contraction values are not shown). The size of the error bars in Figure 3 is an indication of the repeatability of the contraction. A Student's T-test showed distinct differences ($p<0.01$) between high and low signals produced by both the ECR and FCR. In addition, the ratio of the MAV of the agonist to antagonist signal during each contraction was calculated and averaged across similar contractions in order to quantify how much larger the intended signal was over the unintended co-contraction. All of these ratios were greater than one. During low and high ECR contractions, the average ratios were 14.4 and 11.1, respectively. During low and high FCR contractions, the average ratios were 2.5 and 4.8, respectively. Thus, this subject can produce a "purer" ECR contraction (with little FCR co-contraction) than FCR contraction (which elicits a greater degree of ECR co-contraction), as can be seen in Figure 2.

So far the data from this subject seems to suggest that a controller could distinguish whether a command was issued from the FCR or ECR by comparing the levels of the signals from the two muscles. The command could further be distinguished as a high command or low command. Potentially four different neuroprosthesis functions could be assigned to these four different contraction conditions.

A similar analysis will be done for transient contractions. Transient contractions could be used in a control algorithm to switch the system on and off or to toggle between grasp patterns. High or low transients could signal different functions. A time delay would be required in order for a control algorithm to distinguish between a sustained contraction and a transient signal.

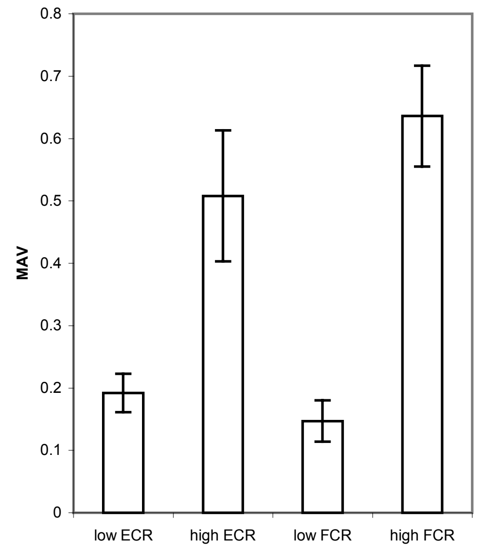

Figure 3: The means and standard deviations of the measurements of the MAV level during low and high contractions of the ECR and FCR. The high signals proved to be statistically greater ($p<.01$) than their low counterparts.

Eliminating Stimulation Artifact

The muscles that will be used for control are in the forearm, physically close to the muscles that will be stimulated to produce hand opening and closing. Therefore, the recording electrodes pick up a strong stimulation artifact due to the electric field generated by the stimulation current. To investigate the characteristics of the stimulation artifact, the myoelectric signal from the ECR during no voluntary contraction was recorded with surface electrodes while the flexor digitorum superficialis (finger flexor) was electrically stimulated with 12.5 Hz (80 ms inter-pulse-interval), 200 μs, 20 mA pulses through a surface electrode. This intensity of stimulation was effective in producing finger flexion. The stimulation artifact picked up by the recording electrodes was found to last about 20 ms for each stimulation pulse. In order to use the volitional myoelectric signals as a control source, the artifact must be eliminated prior to signal processing.

The presence of stimulation artifact in the myoelectric signal can be avoided by blanking the signal during the interval that the artifact will be present. This approach also eliminates the myoelectric signal during those periods, but myoelectric activity recorded outside of the blanking periods is expected to be adequate for use as a control signal, provided the artifact and blanking period are not too long and the stimulation frequency is not too high. Typical stimulation frequencies are 12 and 16 Hz (interpulse intervals of 62 to 83 millisecond). The amplifier we are currently using in these initial trials (Cambridge Electronic Design 1902) is equipped to ground the inputs for a programmable duration in response to a trigger signal, effectively blanking the signal during that interval. With the blanking duration set at 21 milliseconds and triggered 2 milliseconds before each stimulation pulse, the stimulation artifact was effectively eliminated from the myoelectric signal, as shown in Figure 4.

Implementing Control Algorithms

Work has been done to incorporate some control algorithms into the LabView™ data acquisition and signal processing routine and to create an interface that simulates operation of a neuroprosthesis. The control algorithm must enable the user to open and close the hand, maintain the hand in a desired degree of closure, switch between lateral and palmar grasp patterns, and turn the neuroprosthesis on and off. A control algorithm has been implemented that compares the ECR and FCR signals and selects hand opening or closing based on that comparison. If the signal from the FCR is significantly greater than that of the ECR and the FCR signal exceeds a threshold, the neuroprosthesis function selected is hand opening. Conversely, hand closing is selected when the ECR signal is significantly greater than the FCR signal and a preset threshold. Relaxing both muscles below preset levels causes the hand to maintain a position, and strongly co-contracting the muscles causes the grasp to toggle between lateral and palmar grasp patterns. Methods for evaluating the ability of a subject to use this control algorithm and others will be developed in future work.

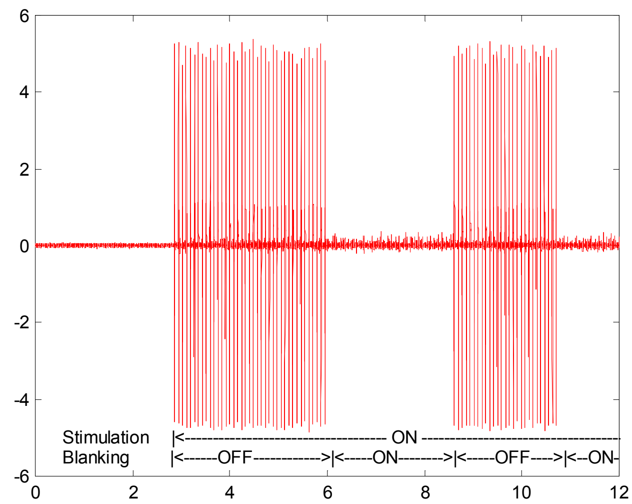

Figure 4: Effectiveness of artifact blanking amplifier.

Next Quarter

With the hardware and software in place for recording myoelectric signals and processing them in real-time, the protocols for recording and quantifying signal characteristics for a given subject will be further refined during the next quarter. A protocol for recording and quantifying the baseline fluctuations of the myoelectric signals in response to external disturbances, changes in arm orientation, and load applied to the hand will be developed. Specifically, the myoelectric signal level required to counteract specific wrist torques expected to be encountered during a hand grasp task must be determine. The ability of a subject to still produce characteristic contractions in loaded conditions will also be defined. Testing on several able-bodied individuals will be carried out using fine-wire percutaneous electrodes for recording.

LabView™ routines will be written for testing the ability of a subject to use a simulated neuroprosthesis governed by a particular control algorithm. Additional routines will be written to interface the stimulator with control algorithms so that the stimulator is governed by the subject's myoelectric signals.

Measurement of human upper extremity nerve diameters and branch-free lengths.

Contract sections:

E.1.a.i Achieving Complete and Selective Activation Via Nerve Cuff Electrodes
E.2.a.i Selective Activation of Elbow and Shoulder Muscles by Nerve Cuff Electrodes

Abstract

The ability to activate selectively individual fascicles of a peripheral nerve trunk using multiple-contact nerve cuff electrodes is well established. In the effort to combine several upper extremity functions into a single neuroprosthesis, we propose to use this technology for activation of specific muscles. Studies of the anatomy, branching patterns, fascicular structure, and surgical access of the upper extremity nerves are necessary so that the sites that maximize the probability of success can be identified. During this quarter we completed the dissection of one set of nerves including measurements of the diameters and branch free lengths of the nerves.

Methods

Dissection was conducted using blunt dissection techniques in a fixed human cadaver. The brachial plexus, its branches, and the branches of the axillary, musculocutaneous, and radial nerve were identified and tagged. Any irregularities were noted and photographed. Length measurements were done using calipers, and the diameters of the branches and nerve trunks were measured using a suture to measure the circumference and assuming a circular cross section. Once these measurements were completed the nerves were excised en masse with muscle branches being tagged with sutures for identification. The nerves were then stored for future studies of fascicular structure.

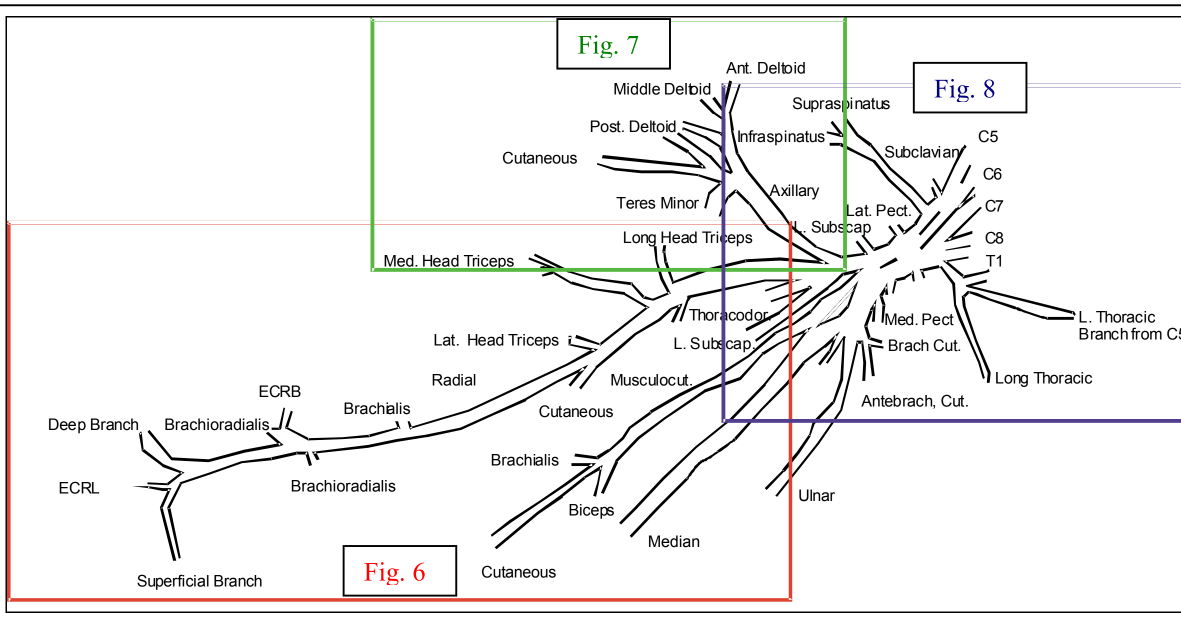

Figure 5: Human right upper extremity nerves (9802R) emerging from the brachial plexus with labeling of terminal branch destinations. The three inset boxes indicate the regions illustrated in Figures 6-8.

Results

The brachial plexus as well as the branches of the axillary, musculocutaneous, and radial nerve are shown in Figure 5. One of the irregularities found involved the innervation of the brachialis. Normally, the brachialis is innervated solely by the musculocutaneous nerve, but in this case, branches to the brachialis were found from the radial and musculocutaneous nerves.

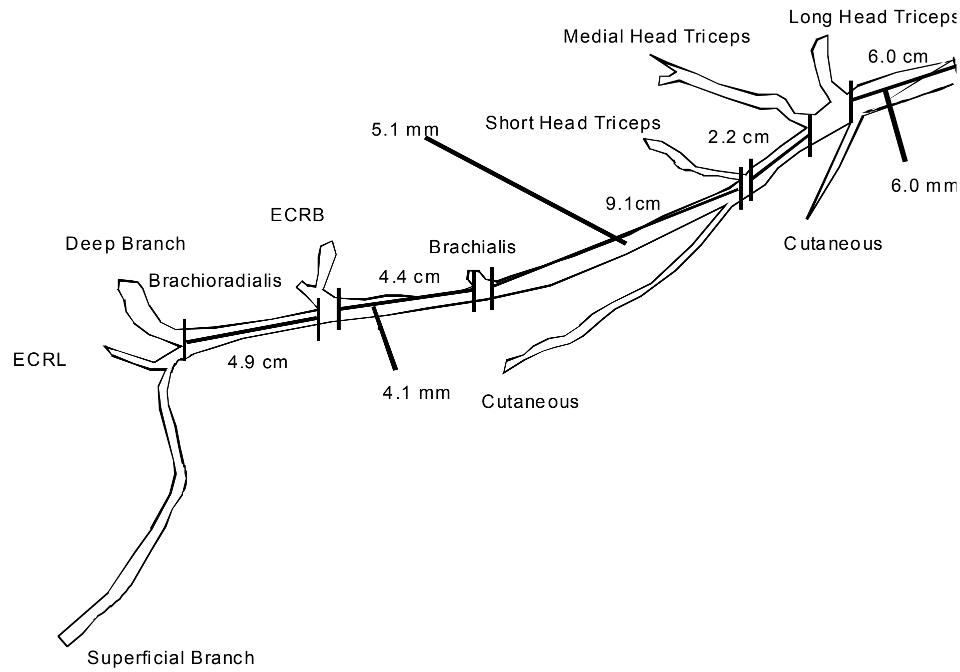

Figure 6. Human radial nerve (9802R) annotated with nerve lengths between branches and nerve diameter measurements.

The other notable irregularity was a branch of the long thoracic nerve that exited the spinal cord from the C5 level. Normally, the long thoracic nerve is made up of branches that all derive from the brachial plexus roots. Also during dissection, the muscle branch innervating the coracobrachialis was not found, but it is believed that this was due to a dissection error rather

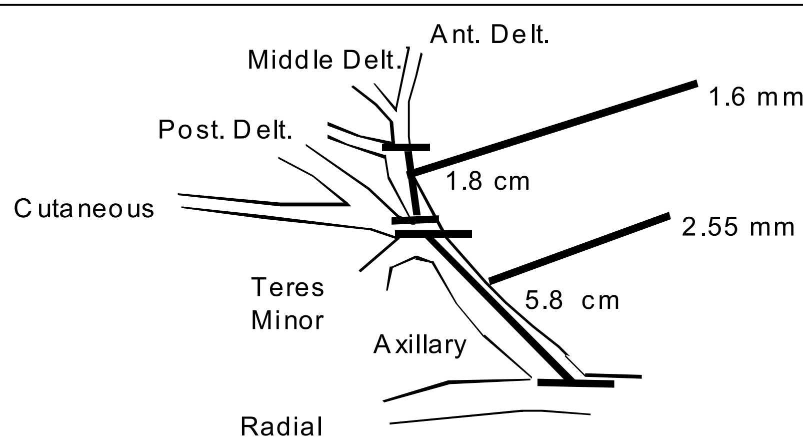

Figure 7: Human axillary nerve (9802R) annotated with nerve lengths between branches and nerve diameter measurements.

then an anomaly. Due to this problem, the results of the musculocutaneous nerve length measurements are incomplete, but the diameter measurements are still complete and the diameter was found to be 2.2 mm prior to the biceps and brachialis muscle branches.

The radial nerve, along with length and diameter measurements of potential nerve cuff electrode sites, is shown in Figure 6, while the same results for the axillary nerve and the brachial trunk are shown in Figures 7 and 8, respectively.

All of the cuff implantation sites that were identified met the minimal criteria for the use of existing multi-contact electrodes. The long thoracic nerve and subclavian nerve were found to have inadequate diameters for the use of existing multi-contact electrodes. Each of these nerves, however, only innervates a one muscle, so single-contact electrodes can be used

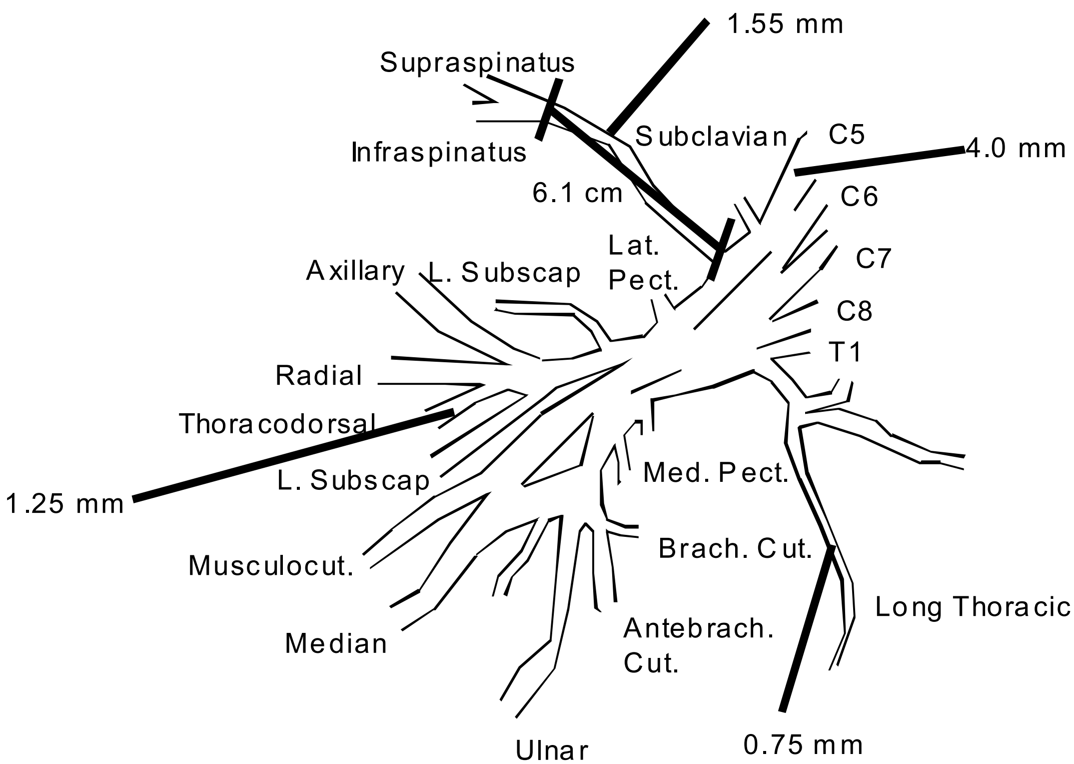

Figure 8: Roots and branches of the human brachial plexus (9802R) annotated with nerve lengths between branches and nerve diameter measurements.

Plans for Next Quarter

During the next quarter, the anatomical study of the upper extremity nerves will continue with the dissection and measurements of additional cadavers being completed. The study of the fascicular structure of these nerve groups will also be underway. A pilot study of the fascicular structure of a radial nerve revealed that cross-sectioning may prove an inadequate method of fascicular mapping due to the large internal structural changes that occur over relatively short length spans. Therefore, the use of lipophilic dyes to retrogradely trace the muscle branches will be pursued.

Magnetic resonance imaging of muscles of the human elbow and shoulder

Contract section: E.1.a.ii.4.1 Model customization: muscle volume estimates via MRI

Abstract

In this project, we are using magnetic resonance imaging (MRI) to non-invasively determine the muscle volume of the shoulder in individuals with high tetraplegia. Muscle volume has been found [Fukunga et al. 1992; Kawakami et al. 1994] to be a good predictor of Physiological Cross Section Area (PCSA) and, hence, maximum muscle force. Individuals with high tetraplegia have extensive paralysis of muscles of the upper extremity, and may have widespread denervation of elbow and shoulder muscles. Characterization of the residual force generating capacity of these muscles, either by voluntary contractions or by FNS of paralyzed muscle fibers, is essential for determining the ultimate feasibility of using FNS in these individuals. It is not reasonable to individually stimulate each of the more than 30 muscles of the shoulder and elbow just to determine the feasibility of a neuroprosthesis, so we will approximate the maximum muscles forces via MRI-based volume measurements.

Methods

Experimental

An able-bodied human subject was placed within an MRI scanner in a supine position. The scanner used was a Siemens Magnetom Sonata, a state-of-the-art 1.5T MRI system with a new, flexible MRI pulse sequence programming language. Both arms were held closely to the side of the thorax to facilitate simultaneous imaging of the muscles of the shoulder and the elbow. The image field of view of the image extended from just below the lower extent of the pectoralis major to the top of the shoulder in the anterior-posterior direction. The lateral field of view was varied in different scans, but included at least the muscles of one shoulder and upper arm. A multi-channel body phased array coil with four active elements was placed in direct contact with the chest wall from just below the neck to the mid-abdomen to improve image signal to noise ratio (SNR). In this first experiment, two potential scanning sequences were explored:

1. 3-D Fast low angle shot acquisition (3D-FLASH with T1 weighting): tip angle of approximately 40^{o}-60^{o}, TE=4 ms, TR=8msec, 256 x 256 x 256 acquisition. Scan time was approximately 9 minutes.
2. 3-D FISP- Imaging parameters were similar to those for item 1 in terms of TE, TR, matrix size and field of view. Due to slightly different methods used to develop contrast between tissues in FISP and FLASH acquisitions, the FISP acquisitions were run at both 20^{0} and 70^{o} excitation angles. The second FISP acquisition was used to assess if a modest amount of T2 weighting could be included into the contrast mechanism to improve contrast between fat and muscle.

Analytical

Our approach for semi-automatic outlining of muscle perimeters consists of four steps: First, manually specify an initial Region of Interest (ROI) that roughly corresponds to the outline of a given muscle within an image slice. Second, perform an automatic contrast search to more finely specify the border of the muscle. Third, interpolate and smooth along the identified border.

Last, carry the border to the adjacent image and start a new round of search. Note that these same procedures are repeated for each muscle of interest.

- Selecting the ROI. This is a manual step that provides the algorithm with an initial, rough estimate of the muscle perimeter in a single image slice. The operator selects a series of points around the perimeter of the muscle using a computer mouse. The algorithm takes the selected pixels to generate a polygon, with the enclosed area defined as the ROI.
- Automatic contrast search. The algorithm then automatically calculates the average pixel intensity and standard deviation within the ROI. Using these two parameters, the algorithm searches areas of the image in proximity to the border of the ROI. If image quality is adequate, the algorithm computes the perimeter of the muscle simply by comparing the pixel intensity of border with the average pixel intensity within the muscle fibers. For those regions where the contrast between the muscle boundaries and the muscular tissue is insufficient, the algorithm retains the operator-selected border and marks the region as a failed-border-search region.
- Interpolation along the border. In the regions of the image where noise has not allowed the muscle border to be located by a simple contrast search, an estimate of the boundary is determined by interpolation of adjacent border areas. If the failed border search in the previous analysis step was due to noise, the failed-border-search pixels will often scatter around the true muscle border and linear interpolation of the pixels across the border region is often successful. However, if a large region of the muscle border cannot be determined by the contrast search, a nonlinear polynomial fit to the successfully identified border regions are used to fill in the unsuccessfully identified regions.
- Smoothing the border. Depending upon the image quality, the contrast search results may not be smooth from point to point along the muscle boundary. The algorithm first detects regions of the border that contains outlier points or small loops, and replaces them using linear interpolation of adjacent points. All the points are then smoothed along the identified border using nonlinear interpolation.
- Carrying the border forward to the next slice. If the operator accepts the automatically determined border, it is carried forward to the adjacent image slice as the initial ROI rather than having this specified manually. Because the images are in sequence and adjacent images often differ only slightly, the algorithm is often able to determine the optimal border of the same muscle on the next image, using the same search algorithm described above. If the automatically selected border is not acceptable, the operator must specify a new manual ROI and repeat the above procedures until an acceptable final border is determined.

Results

In one experimental session, we obtained four sets of complete transverse plane MR images of shoulder and arm, and two sets of sagittal plane images of the same body region. Typically, the transverse plane images will be used for image processing due to the orientations of most shoulder and arm muscles. An example of a transverse image slice is shown in Figure 9.

Several limitations of the initial sets of images were quickly identified. We had attempted to image both shoulders and both upper arms in a single scan to minimize experimental time, but the resulting images were mediocre. Image resolution suffered, movement artifact due to breathing and heart beat distorted a number of the image slices, and image signal to noise ration suffered near the borders of the imaged areas. A second imaging session has already been completed that addressed several of these limitations, and will be described in the next report.

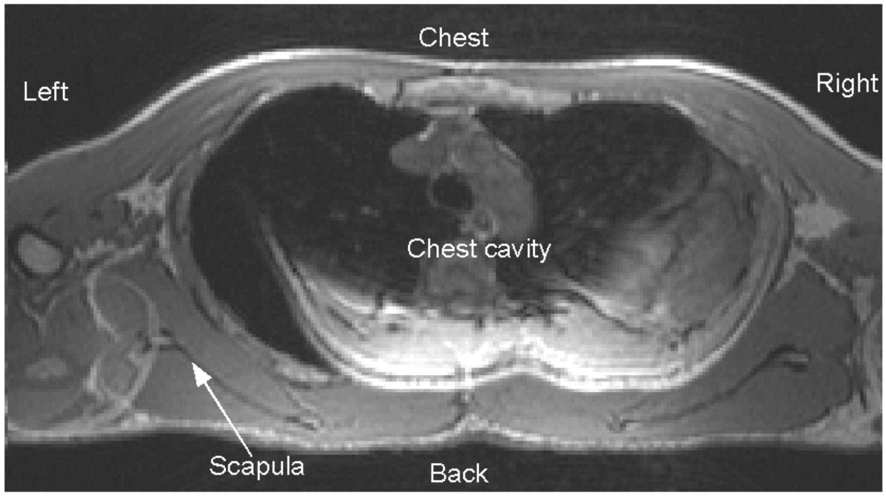

Figure 9: One slice of an MRI scan of the shoulder and upper arm region of a human subject

Most of the effort on this project during this reporting period was devoted to the development of this algorithm. It was found that the algorithm is very effective in identifying borders for regions of interest with relatively good contrast. However, the contrast between muscle tissue and the muscle boundaries in most images from the first session was not sufficient to allow automatic outlining. The function of the algorithm was tested using regions with more prominent borders, such as the upper arm as a whole.

Next quarter:

The limitations in the image quality found in the first session can be easily addressed. A second imaging session was completed just after the end of the quarter. In this experiment, a different subject was used and the imaged area was confined to a single shoulder and upper arm to increase resolution and reduce movement artifact. Longer scans with different parameters were used to increase contrast. Subjectively, the image quality was much improved from the first session. Quantitative data analysis has not yet been performed. Complete analysis of second set of images will be performed to determine if muscle perimeters can be outlined automatically. The semi-automatic search algorithm will be modified as necessary.

References

Fukunaga, T., Roy, R.R., Shellock, F.G., Hadgson, J.A., Day, M.K., Lee, P.L., Kwong-Fu, H., Edgerton, V.R. Physiological cross-sectional area of human leg muscles based on magnetic resonance imaging. *J. Orthop*. Res. 10: 928-934, 1992.

Kawakami, Y., Nakazawa, K., Fujimoto, T., Nozaki, D., Miyashita, M., Fukunaga, T. Specific tension of elbow flexor and extensor muscles based on magnetic resonance imaging. *Eur. J. Appl. Physiol*. 68: 139-147, 1994.